The 21st International Congress on Sound and Vibration

13-17 July, 2014, Beijing/China

PREDICTION OF GROUND VIBRATION FROM TRAINS USING A MULTI-BODY VEHICLE MODEL COUPLED TO A 2.5D FE/BE MODEL OF THE TRACK AND GROUND

Qiyun Jin, David Thompson

Institute of Sound and Vibration Research, University of Southampton, Southampton SO17 1BJ, UK

e-mail: Q.Jin@soton.ac.uk

Ground vibration from trains is a growing environmental problem, especially as the speed and traffic intensity of trains increase. In order to predict vibration, and the influence of vehicle, track and ground parameters, a detailed numerical model is required. A model of the track and ground is presented based on the wavenumber domain finite element / boundary element (FE/BE) method. This so-called 2.5D approach is more efficient than a fully three-dimensional approach. The wavenumber resolution required to achieve good predictions is shown to depend on frequency and the wave speed in the ground. However, for the rail receptance it is necessary to include sufficiently high wavenumbers to capture the static deflection shape. The vehicle is represented by a multi-body model which is coupled to the track through contact springs and excited by the surface roughness. The same roughness excites each wheel/rail contact with appropriate time delay. The effect of different levels of detail in the vehicle model is studied as well as the influence of coupling between the contact points through the track/ground model. Results are presented for an example track and ground and they show good agreement with other modelling approaches.

1. Introduction

Ground vibration generated by trains running on railway tracks can lead to annoying disturbance, such as feelable vibration and ground-borne noise within the buildings nearby.[1] The prediction of this train-induced vibration is extremely important for parametric study and mitigation design. Many theoretical models have already been developed to date.[2-6]

Analytical models allow fast numerical computations and are able to take account of an infinite domain.[2,3] The FE-BE method is also favoured in modelling the train-induced vibration owing to its flexibility in dealing with the arbitrary geometry of structures and interfaces in the ground. A comparison between 2D and 3D models showed that although the 2D model had a lower computational cost, its results differed from the full 3D ones to a certain degree.[4] As a compromise, a so-called 2.5D methodology developed initially by Aubry et al.[5] has grown in popularity. Based on this approach, a numerical model was built by Sheng et al. to predict the ground vibration induced by trains either running on the ground surface or in a tunnel.[6] In this paper, an existing program called WANDS (Wave-Number-Domain FE-BE Software)[7] which is based on the 2.5D method is used to

model the track and ground. By coupling this with different vehicle models, the rail and ground vibrations induced by surface trains are studied over a frequency range from 1 to 100 Hz.

2. 2.5D methodology

The 2.5D methodology is a wavenumber-based approach, in which a 2D FE-BE mesh is used to solve the response within a cross-section, while the longitudinal direction, which is assumed to have longitudinally invariant geometry, is solved in the wavenumber domain.

By solving displacements at the nodes (y, z) of the 2D FE-BE model for each frequency (ω) and wavenumber (β), an inverse Fourier transformation with respect to the wavenumber is employed to retrieve the solution in the longitudinal direction (or x-direction). In practice, the integration over a continuous infinite range of wavenumbers is replaced by a summation over discrete equally spaced wavenumbers within the range defined by a maximum wavenumber ($\beta_{\max}$):

$$\hat{u}(x,y,z,\omega) = \frac{1}{2\pi}\sum_{-\beta_{\max}}^{\beta_{\max}} \tilde{u}(\beta,y,z,\omega)e^{-i\beta x}\Delta\beta \tag{1}$$

where $\hat{u}$ and $\tilde{u}$ are the displacement functions in space and wavenumber domain, respectively.

The wavenumber spacing (or resolution) $\Delta\beta$ and the maximum wavenumber ($\beta_{\max}$) are two parameters given in the WANDS input which should be properly chosen to ensure reliable results.

3. Model description

In order to study the train-induced vibration, a modelling system was constructed, which consists of three subsystems: the track/soil subsystem, the train subsystem and the coupling subsystem.

3.1 Track/ground subsystem

The track and ground is modelled using WANDS[7] as shown in Figure 1. The ground, based on a site at Horstwalde in Germany, is assumed to be homogeneous and is modelled with boundary elements. Ground layers could also be included if needed. The ballasted track is located directly on the ground surface. The rails are modelled as Euler-Bernoulli beams, and the rail pads, sleepers and ballast as solid elements. The parameters of the ground and track are listed in Table 1. The parameters of rail and rail pad are given per rail, and the stiffness of the rail given in the table is bending stiffness. A unit force is divided into four and applied on the two nodes of each rail element.

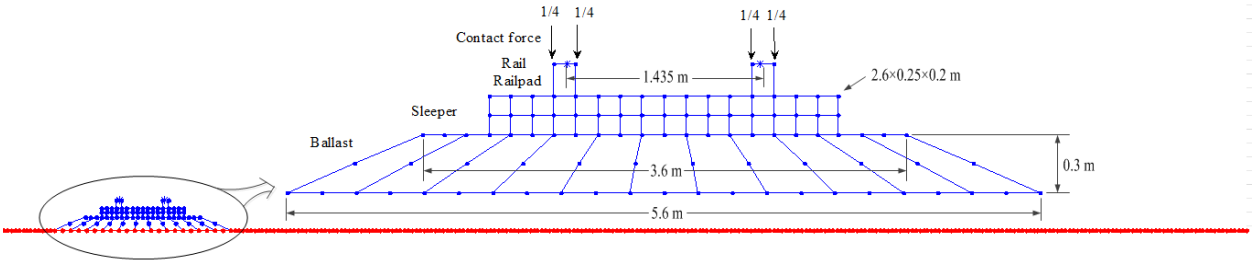

Figure 1. 2D FE-BE cross-section of track and ground model in WANDS

Table 1. Soil properties of example ground and parameters of track

Ground	Shear wave speed	Dilatation wave speed	Loss factor	Density
	250 m/s	1470 m/s	0.05	1945 k/m^3

	Mass *per unit length*	Stiffness *per unit length*	Damping loss factor
Rail	60 kg/m	6.4×10^6 Nm^2	0.01
Sleeper / rail pad	542 kg/m	5×10^8 N/m^2	0.1
Ballast	1740 kg/m	4.64×10^9 N/m^2	0.04

The third direction of the track/ground model is formed in the wavenumber domain as explained with equation (1). A sufficient number of wavenumbers has to be calculated, so that the wavenumber resolution ($\Delta\beta$) is fine enough to capture the peaks in the transfer function while the wavenumber range defined by the maximum wavenumber ($\beta_{\max}$) should cover all the influential waves for the frequencies of interest. The number of wavenumbers calculated in this model is chosen to be 1024. Several different combinations of $\Delta\beta$ and $\beta_{\max}$ are used to study their influence.

3.2 Train subsystem

The train is modelled as a set of multi-body vehicles. Three types of vehicle model are considered, as shown in Figure 2: an unsprung mass model (1dof), a quarter car (3dof), and a four-wheelset model (10dof). The two wheels in a wheelset are treated as a single degree of freedom. m_w, m_b, m_c are the masses of wheelset, bogie and carbody; k_{s1}/c_{s1}, k_{s2}/c_{s2} are the stiffness and damping of primary and secondary suspensions. The parameters are listed in Table 2.

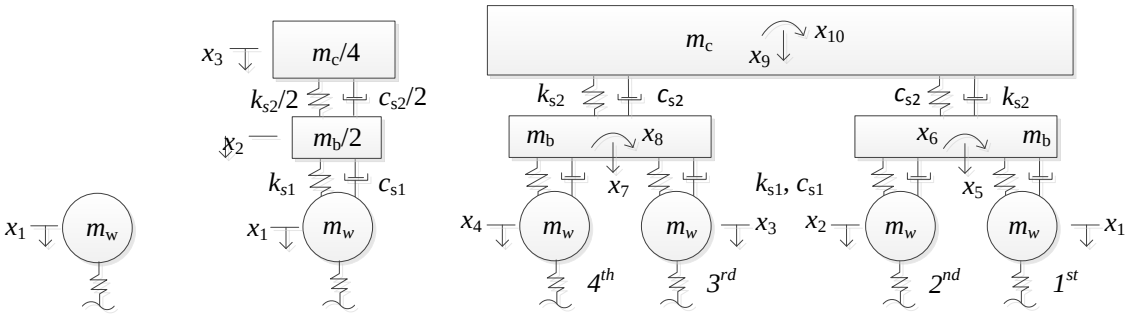

Figure 2. Three types of vehicle model

Table 2. The parameters of a vehicle[8]

m_c	m_b	m_w	k_{s1}	k_{s2}
40,000 kg	5000 kg	1800 kg	2.4×10^6 N/m	6.0×10^5 N/m
J_c	J_b	k_H	c_{s1}	c_{s2}
2.0×10^6 kg.m^2	6000 kg.m^2	2.925×10^9 N/m	3.0×10^4 Ns/m	2.0×10^4 Ns/m

The displacement vector is given by $\{x\}=\{x_1\ x_2\ \ldots\ x_m\}^T$, where m=1, 3 or 10. For harmonic motion at frequency ω, the displacements are related to the force vector $\{F\}$ by the mobilities:

$$i\omega\{x\} = [Y_w]\{F\} \tag{2}$$

For the 3dof and 10dof models, $Y_w = \left(-\omega^2[M]+i\omega[C]+[K]\right)^{-1}$ in which $[M]$, $[C]$ and $[K]$ are mass, damping and stiffness matrices respectively.[2] For the 1dof model, $Y_w = -i/m_w\omega$.

The 1dof and 3dof models have a single wheelset, the mobility of which is a single function of frequency, whereas for the 4-wheelsets model (10dof), the vehicle mobility is a 4×4 matrix. However, the full vehicle mobility (4×4 matrix) of the 1dof and 3dof models can be easily assembled by $Y_w^{veh} = Y_w I_{4\times4}$ where I is the unit matrix. The mobility of the whole train can be formed:

$$Y_{train} = \begin{bmatrix} Y_w^{veh} & & 0 \\ & \ddots & \\ 0 & & Y_w^{veh} \end{bmatrix}_{4n\times4n} \tag{3}$$

where n is the number of vehicles within the train.

3.3 Coupling system

The wheel and track are excited by the vertical roughness between them. The roughness spectrum of the track is chosen as a standard FRA class 3 spectrum. Neglecting the roughness of the wheel profile, each contact point experiences the same roughness apart from a time delay. If the roughness spectrum at one wheel/rail position is r, the roughness spectra for all the contact points, $R = r \times T_r$ where the time delay vector T_r can be expressed as:

$$T_r = \{e^{-i\omega x_0(1)/v} \quad e^{-i\omega x_0(2)/v} \quad \cdots \quad e^{-i\omega x_0(j)/v} \quad \cdots \quad e^{-i\omega x_0(n_w)/v}\}^T \tag{4}$$

where j=1, 2, …, n_w is the number of wheelsets, v is the speed of train, x_0 is the vector of wheelset positions. Using this roughness vector, the equation of motion of the wheel-rail system is:

$$\left[Y_r + Y_{train} + Y_c\right]_{4n\times 4n}\{F\} = \{T_r\} i\omega r \tag{5}$$

where Y_r and Y_{train} are mobility of rail and train solved from the subsystems above, $Y_c=i\omega/k_H$ is the mobility of contact spring, k_H is the stiffness of a Hertzian spring (given in Table 2) for two wheels.

From equation (5), the contact forces can thereby be found. Combining the contact forces with the rail and ground mobility, the train-induced vibration can be obtained:

$$\{v_g\} = \left[Y_g\right]\left[Y_r + Y_w + Y_c\right]^{-1}\{T_r\} i\omega r \tag{6}$$

where $\{v_g\}$ are the vibration velocities of the rail or ground, and $[Y_g]$ are the track or ground transfer mobilities, obtained from the track/ground model.

4. Results and analysis

Using the coupled train/track model and the parameters given above, the contact forces between wheel and rail, and the rail and ground vibration induced by a running train have been calculated. These results have been verified by comparison with other prediction models and measurements (not presented here). In this section, the importance of the wavenumber resolution and maximum wavenumber used in the calculation will be indicated. In addition, the effect of different vehicle models and the matrix size of rail mobility used in the coupling system will also be analysed.

4.1 Rail and ground receptance

Based on the results from the example track/ground model, the influence of the two parameters (β_{max} and $\Delta\beta$) in the wavenumber domain is explained.

The rail receptance is plotted against the wavenumber at certain frequencies in Figure 3. The receptance reduces rapidly after a peak, and beyond a certain wavenumber range the value becomes less influential in the integration of equation (1). Figure 4 shows the rail receptance obtained by using different maximum wavenumbers in the calculation. As β_{max} increases from 1.0 to 6.4 rad/m, the rail receptance gradually converges to the correct value for all frequencies. Figure 5 shows the ground receptance due to an excitation force on the ground surface. The peaks, as in Figure 3, are related with the Rayleigh wave, the most significant wave propagating on the ground surface. The wavenumber at the peak increases with the excitation frequency. Extracted from the curves for each frequency between 1 and 100 Hz, the wavenumber of the peaks forms a straight line in the dispersion diagram, as shown in Figure 6. Also shown are the theoretical wavenumbers of the Rayleigh wave and shear wave in the example soil. The speed of the Rayleigh wave is 95% of the shear wave speed. The dispersion curve obtained from the peak wavenumbers from the wavenumber spectra is identical with the theoretical result for the Rayleigh wave, which confirms that the peak corresponds to the Rayleigh wave. If the maximum wavenumber is more than twice the wavenumber of the Rayleigh wave, the wavenumber range should cover all the influential waves.

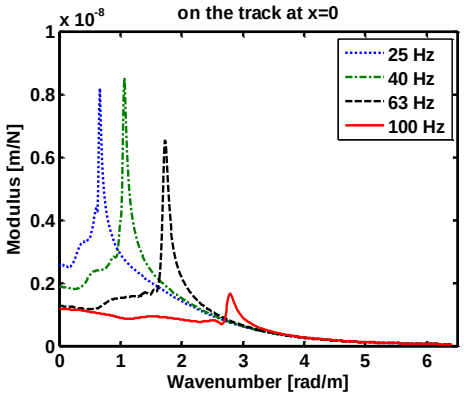

Figure 3. Rail receptances against wavenumber at different frequencies

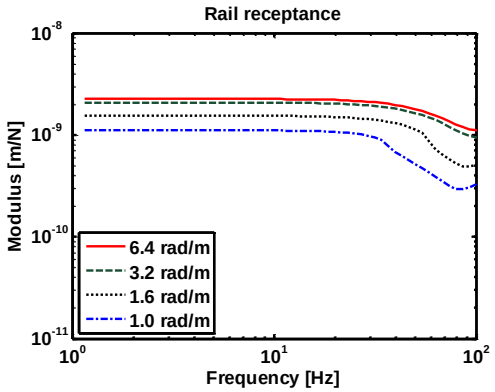

Figure 4. Rail receptances obtained using different maximum wavenumbers

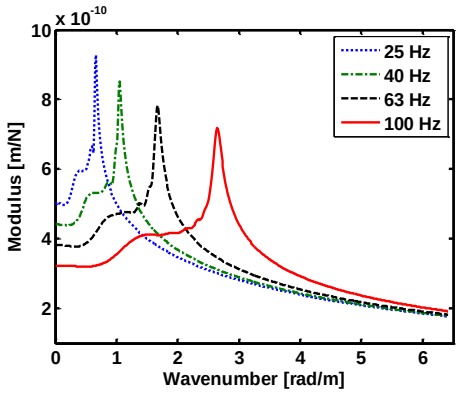

Figure 5. Point receptance of ground against the wavenumber at different frequencies

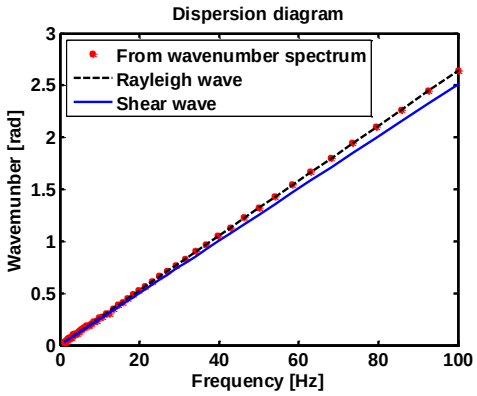

Figure 6. Dispersion diagram

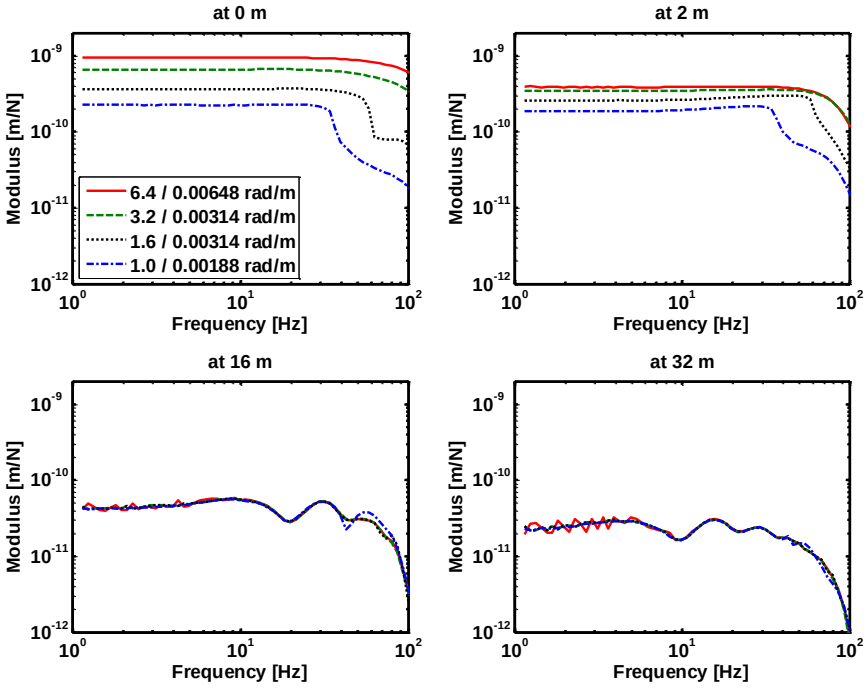

Figure 7. Transfer receptance from the track to the ground at different distances with different β_{max} and $\Delta\beta$

The transfer receptance from the track to the ground at different distances is plotted in Figure 7. Different combinations of maximum wavenumber and wavenumber resolution are used in the calculation. Similar to the rail in Figure 4, a significant inaccuracy occurs for distances near to the

track (at 0 m and 2 m) with insufficient maximum wavenumber. This shows that the near-field around the force contains a much wider range of wavenumbers even for low frequencies. However, the differences gradually disappear as the distance increases, although the influence of β_{max} can still be seen for high frequencies. Besides, at distances of 16 m and 32 m, the fluctuations at the low frequencies indicate that the wavenumber resolution used is too coarse for these frequencies.

4.2 Difference between vehicle models

Different vehicle models are introduced (see Figure 2) and coupled with the track to find the contact forces. The wheel mobility for each model is shown in Figure 8, where the differences mainly exist below 10 Hz. The mobility of the 1dof model is controlled by the unsprung mass. Below 8 Hz, the mobility of the 1dof model is the highest of the three. The peaks and dips for the 3dof and 10dof models are caused by the primary and secondary suspensions within the multi-body vehicle. Due to the inclusion of rotation in the bogie and car body, the mobility of the 10dof model differs slightly from that of the 3dof model, with the frequencies of the peaks being shifted.

Figure 9 shows the contact force spectra obtained from the coupled vehicle/track system by using the different vehicle models. Influenced by the wheel mobility in Figure 8, the difference between these contact forces also exists at frequencies below 10 Hz where the multiple dof models give a higher contact force than the 1dof model. Above 10 Hz, the type of vehicle model used has no influence on the results. Therefore, it can be concluded that the suspensions within the vehicle model are influential at frequencies below 10 Hz, while they have no impact for higher frequencies.

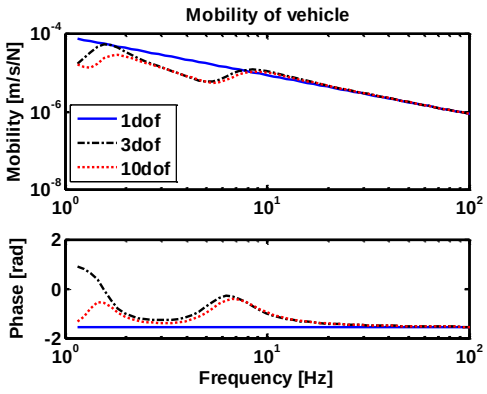

Figure 8. Wheel mobility of 1dof, 3dof and 1st wheel of 10dof model

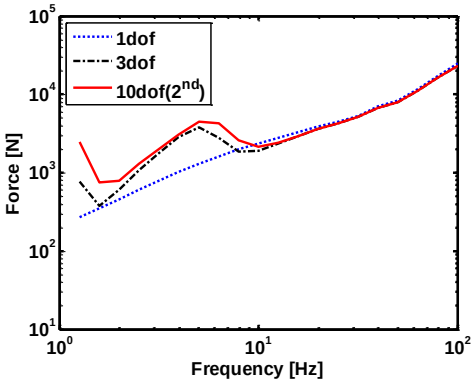

Figure 9. Contact forces obtained by using different vehicle models

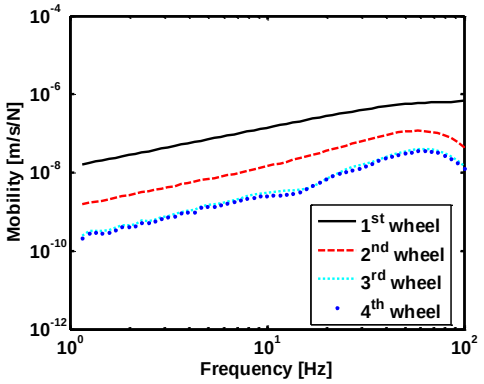

Figure 10. Rail mobility at four wheel positions of a vehicle to the excitation at 1st wheel position

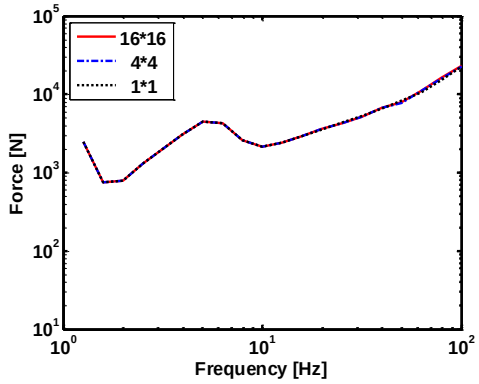

Figure 11. Contact force obtained with different rail mobility matrices

4.3 Different matrix size of rail mobility

The rail mobility is obtained from the WANDS model. For each wheel position in a vehicle,

the point and transfer mobility to a force at the 1st wheel position on the rail are shown in Figure 10. The difference between these rail mobilities is approximately independent of frequency.

In the same way as for the vehicle, the rail mobility can also be constructed with different degrees of complexity. For example, the rail mobility for a single wheelset (1×1 matrix) consists only of the point mobility, while the rail mobility of a vehicle range (4×4 matrix) includes the transfer mobility of the other wheelset positions within a vehicle length. The contact forces solved using the rail mobility matrices of different complexity are shown in Figure 11. The 16×16 matrix is the rail mobility of a full train range (a four-vehicle train). No evident difference is found among the results, as rail vibration decays rapidly with distance. Therefore, the single point mobility is sufficient.

4.4 Train-induced vibration

Using the WANDS model coupled with the 10dof vehicle model, the rail and ground vibration induced by a train running at 150 km/h has been predicted. The quasi-static component of vibration corresponds to the deflections under the axle load moving with the passage of the train, while the dynamic component is due to the train-track interaction caused by the excitation mechanisms which is solely the rail roughness in this paper.

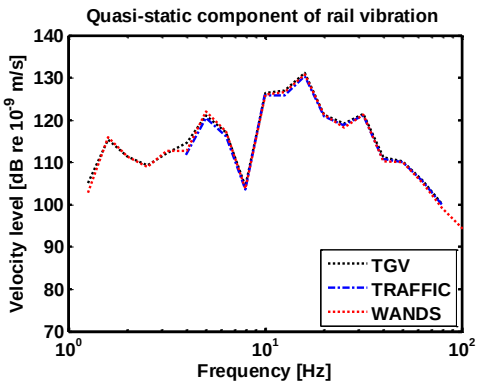

Figure 12. Quasi-static component of rail vibration

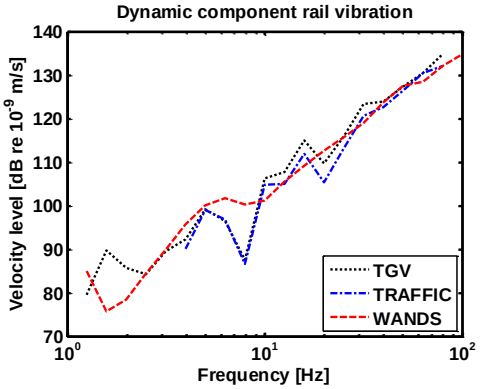

Figure 13. Dynamic component of rail vibration

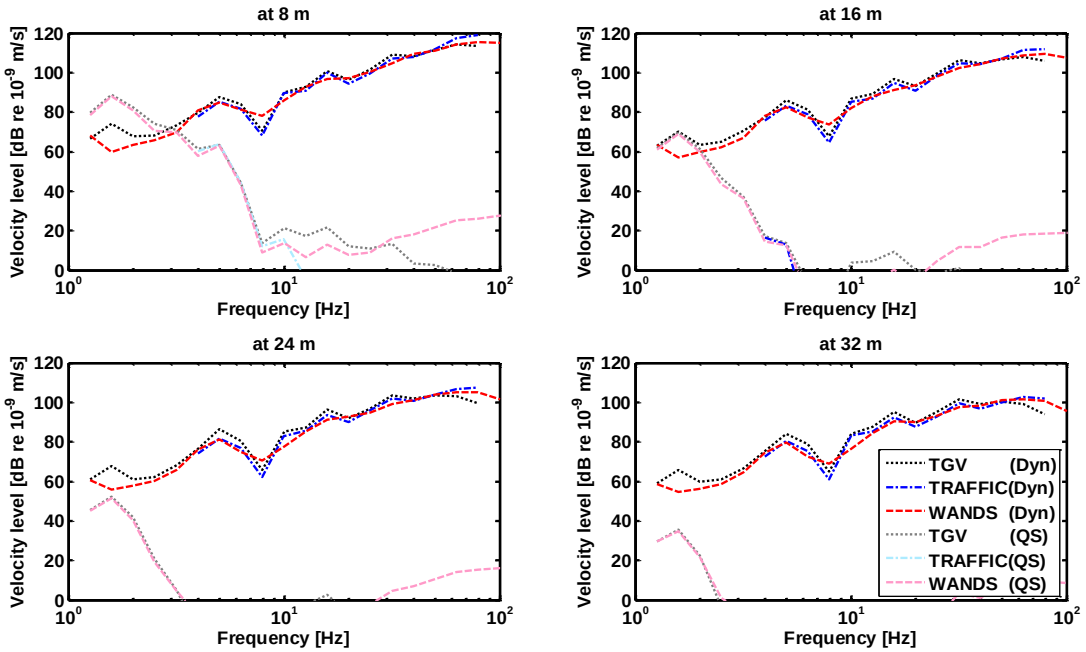

Figure 14. Ground vibration (Dyn: dynamic component; QS: quasi-static component)

The quasi-static and dynamic rail vibrations obtained from WANDS, TGV[2] and TRAFFIC[9] models are compared in Figure 12 and Figure 13. The results given by WANDS are averaged over

the train length. The calculation results from the TGV and TRAFFIC models are based on the same parameters. TGV is an analytical model given by Sheng, while TRAFFIC is a numerical model developed by KU Leuven, results from which were provided in the RIVAS project. Excellent agreement is shown in the quasi-static components. For the dynamic components, the result of WANDS is much smoother as the vehicle is not actually moving along the track. However, the trend is predicted correctly. Figure 14 shows the quasi-static and dynamic components of ground vibration from the different models in bright and light colours respectively. Good agreement is found between these calculation results. The quasi-static component of vibration decays rapidly with the increase of distance from the track.

5. Conclusions

The coupling of a 2.5D track/ground model with multi-body vehicle models is presented in this paper. With this model, the rail and ground vibration induced by a running train can be determined. The parameters used in the wavenumber domain are vital for the 2.5D track/ground model, which should be carefully chosen according to the soil properties and frequency range. A wider range of wavenumbers is required to model the rail and near-field vibration, while for the far-field, the maximum wavenumber needed is less onerous and depends on the excitation frequency. However, for the low frequencies, attention has to be paid to the wavenumber resolution, which should be fine enough to capture the peak in the discontinuous discretized integral functions.

From the contact forces solved from the coupled system, the vehicle models and rail mobility with different complexities are studied. Three different vehicle models show differences below 10 Hz. Above this frequency, the simplified unsprung mass model is sufficient. For the rail mobility, the transfer mobility at the other wheelset positions has negligible effect for the coupling system.

In the comparison with other calculation results of rail and ground vibration, the correctness of the model proposed in this paper has been verified.

References

1. Jones, C. J. C., Thompson, D. J. and Petyt, M. A model for ground vibration from railway tunnels, *Proceedings of the Institution of Civil Engineers-Transport*, **153**, 121-129, (2002).
2. Sheng, X., Jones, C. J. C. and Thompson, D. J. A theoretical model for ground vibration from trains generated by vertical track irregularities. *Journal of Sound and Vibration* **272**(3), 937-965, (2004).
3. Hussein, M. and Hunt, H. A numerical model for calculating vibration from a railway tunnel embedded in a full-space, *Journal of Sound and Vibration*, **305**, 401-431, (2007).
4. Andersen, L. and Jones, C. J. C. Coupled boundary and finite element analysis of vibration from railway tunnels—a comparison of two-and three-dimensional models, *Journal of Sound and Vibration*, **293**, 611-625, (2006).
5. Aubry, D., Clouteau, D. and Bonnet, G. Modelling of wave propagation due to fixed or mobile dynamic sources, *Workshop Wave*, 109-121, (1994).
6. Sheng, X., Jones, C. J. C. and Thompson, D. J. Modelling ground vibration from railways using wavenumber finite-and boundary-element methods. *Proceedings of the Royal Society A: Mathematical, Physical and Engineering Science* **461**, 2043-2070, (2005).
7. Nilsson, C. M. and Jones, C. J. C. *Theory manual for WANDS 2.1*, ISVR Technical Memorandum No. 975. University of Southampton, 2007
8. Mirza, A. A., Frid, A., Nielsen, J. C. O. and Jones, C. J. C. Ground vibrations induced by railway traffic - the influence of vehicle parameters, *Proceedings of the 10th International Workshop on Railway Noise IWRN10*, Nagahama, Japan, October, (2010).
9. Lombaert, G., Degrande, G., Kogut, J. and François. S. The experimental validation of a numerical model for the prediction of railway induced vibrations, *Journal of Sound and Vibration* **297**.(3), 512-535, (2006).